Synthesis and investigation of superheavy elements: perspectives with radioactive beams

Gottfried Münzenberg

Email alerting service	Receive free email alerts when new articles cite this article - sign up in the box at the top right-hand corner of the article or click **here**

To subscribe to *Phil. Trans. R. Soc. Lond. A* go to: **http://rsta.royalsocietypublishing.org/subscriptions**

THE ROYAL
SOCIETY

Synthesis and investigation of superheavy elements: perspectives on radioactive beams

By Gottfried Münzenberg

*Gesellschaft für Schwerionenforschung mbH, Planckstr. 1,
D64220 Darmstadt, Germany*

The perspectives for the investigation of heavy and superheavy elements with intense beams of radioactive nuclei available from the new generation of secondary beam facilities in combination with modern experimental developments are the subject of this paper. The nuclear properties of the recently discovered shell nuclei centred at $Z = 108$ and $N = 162$ and predictions on the location of the superheavy region with improved theoretical models are discussed.

Keywords: superheavy elements; heavy-ion fusion; new elements;
naming of elements; shell stabilization; separation in flight

1. Introduction

(a) Superheavy nuclei: the extension of the chemical elements

The creation of three new elements (Hofmann *et al*. 1995*a*, *b*, 1996), with proton numbers 110, 111, and 112 close to the predicted superheavy proton shell closure $Z = 114$, and the new generation of radioactive beam facilities providing accelerated secondary beams of neutron-rich nuclei and new high-current accelerators (Münzenberg 1998), open interesting new possibilities for superheavy element research. The discovery that the heaviest known elements belong to a region of shell-stabilized, deformed nuclei (Armbruster 1985*a*; Münzenberg *et al*. 1985), centred at $Z = 108$ and $N = 162$ already located in the region of macroscopic instability (Patyk & Sobiczewski 1991), motivated a series of theoretical calculations with macroscopic–microscopic and recently also with self-consistent methods (Cwiok *et al*. 1996; Rutz *et al*. 1997).

Of fundamental interest in heavy-element research is the exploration of the limits of nuclear stability towards the heaviest nuclei and the question of how many elements could exist in nature. A first answer was given by Meitner & Frisch (1939) immediately after the discovery of nuclear fission by Hahn and Straßmann, when they explained the fission process in terms of the disintegration of a charged nuclear droplet. The limits for the existence of heavy nuclei are determined by the delicate balance of the Coulomb repulsion between the large number of protons and the attractive nuclear forces. Consequently, spontaneous fission is decay-mode-specific to the elements at the top of the nuclear table, uranium and beyond. Meitner & Frisch estimated that the periodic table would end at about element $Z = 100$. Detailed investigation of the fissioning nuclear droplet by Bohr & Wheeler (1939) and Feenberg (1939) located the upper end of the periodic table close to 110 protons.

The question arose as to whether shell stabilization could be strong enough to extend the nuclear table beyond the macroscopic limit into the new region of super-
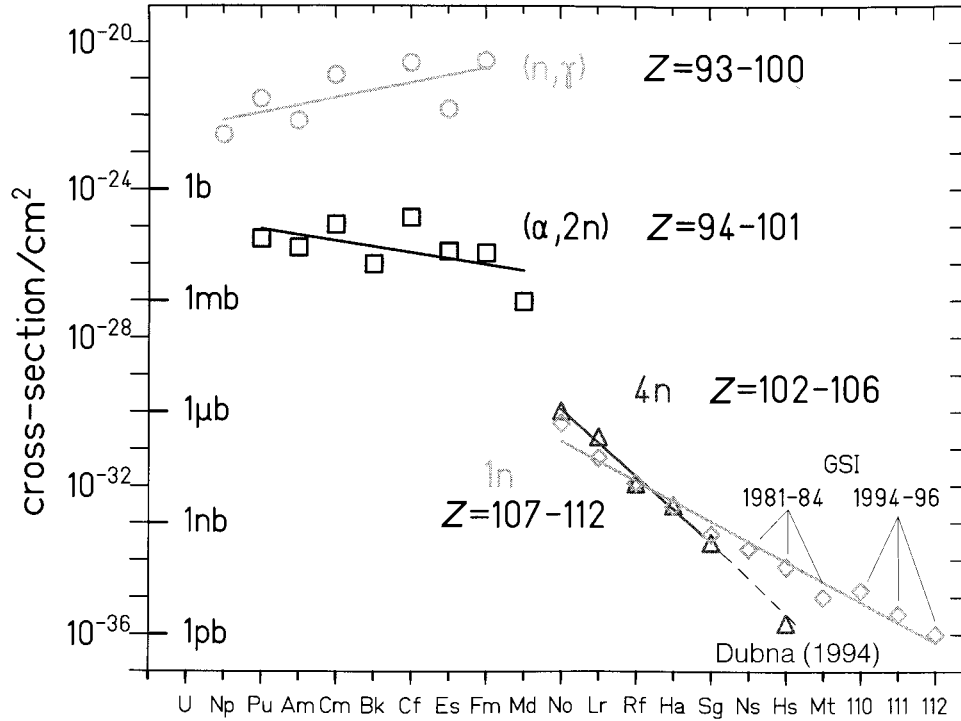
TEX Paper

Figure 1. Synthesis reactions and production cross-sections for the artificial elements beyond uranium.

heavy nuclei. Several calculations performed by Mosel & Greiner (1969), Fizet & Nix (1972), Randrup *et al.* (1974), to give some important examples, predicted an island of superheavy nuclei at the double-shell closure $Z = 114$ and $N = 184$, well separated from the upper end of the periodic table by a sea of fission instability. The predicted half-lives ranged up to 10^9 years, long enough for superheavy nuclei to exist in nature (Fizet & Nix 1972).

(*b*) *Production of transuranium elements*

The next elements beyond uranium are created by breeding in nuclear reactors. By neutron capture and subesequent β-decay, it is possible to climb up element by element until this path is closed by fission which occurs at fermium. All of the transfermium elements, these are the elements $Z = 101$ and beyond, are produced by complete fusion of heavy ions (Seaborg & Loveland 1990; Armbruster 1985*a*; Münzenberg 1988, 1995; Hofmann 1997). Figure 1 compiles the production cross-sections. For complete fusion, they are far below the geometric cross-section, in contrast to those for neutron capture, and drop quickly below the nanobarn level towards the heaviest elements.

Two types of reactions have been used successfully so far. Actinide targets close to the element to be produced were irradiated with light beams ranging from carbon to sulphur, and the fusion of lead or bismuth targets with correspondingly heavier beams ranging from calcium to zinc. This second type of reaction leads to cold

compound systems (Oganessian 1974), and has been used as the only successful route to synthesize the heaviest elements known at present. Both synthesis reactions have in common small production cross-sections dropping to the order of picobarns for the heaviest elements. The respective production rates with present techniques count in atoms per day or even per week.

Upgraded and new radioactive beam facilities producing intense exotic nuclear beams with energies above the Coulomb barrier will provide neutron-rich beams for heavy-element research (Geissel *et al.* 1995; Kubono 1997). Existing laboratories such as GANIL (Caen, France), RIKEN (Tokyo, Japan) and its upgrade (RIKEN 1994), MSU (East Lansing, USA) and its upgrade, and GSI (Darmstadt, Germany) and its upgrade are based on the fragmentation of relativistic projectile beams and are less suited for heavy-element production due to the high-beam energy being far above the Coulomb barrier. A new generation of planned and starting facilities is based on the acceleration of radioactive beams from on-line separators to energies close to the Coulomb barrier. Those are SPIRAL of GANIL (SPIRAL 1994), EXCYT (Catania, Italy), Oak Ridge (USA), Argonne (USA) (Argonne 1995), INS (Tokyo, Japan) and the reactor-based facilities PIAFE (Grenoble (the PIAFE project has been stopped)), and the Munich Project (Germany). The expected intensities are $10^7 \, \text{s}^{-1}$ for the running, and up to $10^{12} \, \text{s}^{-1}$ for the projected facilities, close to $5 \times 10^{12} \, \text{s}^{-1}$ used at present for heavy-element synthesis. New high-current accelerators for beams of stable nuclei will provide beams of up to $10^{15} \, \text{s}^{-1}$, necessary to proceed beyond element 114.

In the experiments with stable beams, only neutron-deficient isotopes of the heaviest elements could be produced. Element 112 is fairly close to the spherical proton shell, but the discovered isotope with mass 277 is still far away from the magic neutron number. Radioactive neutron-rich beams will allow us to approach the spherical $N = 184$ region. To profit fully from the new possibilities of synthesizing heavy and superheavy elements, new reactions such as the hitherto unexplored fusion of symmetric systems (reversed fission) and the importance of isospin and shell effects need further exploration. The discovery of sufficiently long-lived nuclides in the shell region interconnecting the transuranium and the superheavy elements opens up the possibility of investigating the structure of the new species of closed-shell nuclei in the transition region from deformed to spherical.

Moreover, several new experimental developments, such as in-flight separation, efficient 4π germanium detectors, and ion traps, will give new access to nuclear and atomic structure. The expected long half-lives of the neutron-rich species that can be produced with radioactive beams open up possibilities of chemical investigations, which will be addressed briefly.

2. Recent experimental results: our present understanding of superheavy nuclei

(*a*) *Nuclear properties*

Heavy-element research at the very limits of nuclear stability is physics with single atoms. Safe and background free identification of individual atoms allows one to extract gross properties (Münzenberg *et al.* 1984*a*; Geissel *et al.* 1995) such as dominant decay modes, half-life, decay energy, and mass. Even ground-state deforma-

tions can be evaluated (Münzenberg 1995). With the inclusion of theoretical models, experimental shell-correction energies, fission barriers and ground-state deformations have been obtained (Münzenberg 1988, 1995).

In this section, recent experimental results of importance for our understanding of the properties of the elements at the top of the nuclear table are summarized. More details are given in several reviews (Seaborg & Loveland 1990; Armbruster 1985a; Münzenberg 1988, 1995; Hofmann 1997). Our present knowledge on the decay properties of the heaviest elements is summarized in figure 2, which shows the upper part of the chart of nuclides with the observed decay modes, half-lives, α-decay energies, and branching ratios.

The name symbols are given as accepted by CNIC (Greenwood 1997) based on the proposals of the discoverers. CNIC is the commission for nomenclature of the International Union of Pure and Applied Chemistry (IUPAC), preparing the name proposals for the plenary meeting in August 1997. It has set the following: Db for dubnium ($Z = 104$), Ha for hahnium ($Z = 105$), Sg for seaborgium ($Z = 106$), Bh for bohrium ($Z = 107$), Hs for hassium ($Z = 108$) and Mt for meitnerium ($Z = 109$). For elements 110, 111 and 112, no names have so far been proposed. These names have been approved by the IUPAC.

The observation of α-decay as the prominent decay mode of element 106 indicated for the first time an enhancement of stability against spontaneous fission (Demin *et al.* 1984; Münzenberg *et al.* 1985). This was in contrast to the early results and extrapolations, where all even–even isotopes beyond hassium were predicted to fission with half-lives of microseconds or less (Randrup *et al.* 1976). The experimental results on the stability of element 106 against fission indicating the onset of a microscopic stabilization dramatically changed our understanding of the heaviest elements.

Element 108 was identified in the reaction ^{208}Pb(^{58}Fe,n)^{265}108 on the basis of three atoms (Münzenberg *et al.* 1984b, 1987a, b), and confirmed in a later experiment, where 75 α-decays of this isotope were observed in the same reaction (Hofmann *et al.* 1995a). The isotope ^{264}108 is the heaviest doubly even nucleus known at present; it decays by α-decay and spontaneous fission (Münzenberg *et al.* 1987b; Hofmann *et al.* 1995b). The isotope ^{267}108 was produced in irradiations (Lazarev *et al.* 1995) of ^{238}U with ^{34}S and confirmed (Hofmann *et al.* 1995a) when it appeared as the daughter in the decay chain of ^{271}110. The half-lives range from 0.45 ms for the doubly even isotope with mass 260 to 9.3 s for the most neutron-rich isotope with mass 269.

Element 109 was first observed in irradiations of ^{209}Bi with ^{58}Fe by measuring the α-decay chain originating from a single atom. It was assigned to the isotope with mass 266 on the basis of a careful statistical analysis of the decay sequence (Münzenberg *et al.* 1982, 1984a), a result confirmed in later experiments (Münzenberg *et al.* 1988; Hofmann *et al.* 1997). The isotope ^{268}109 was discovered (Hofmann *et al.* 1995b) in the decay chain from element 111. The half-lives of the two α-emitting isotopes are 3.4 ms and 70 ms, respectively. At present, altogether 13 atoms of element 109 have been produced, not counting those appearing in decay chains.

Element 110 was produced (Hofmann *et al.* 1995a) in the reaction ^{208}Pb(^{62}Ni,n) by the identification of the isotope ^{269}110. The more neutron-rich isotope ^{271}110 was synthesized by using a ^{64}Ni beam. The production cross-section was 15 pb and enhanced by a factor of about four as compared to the ^{62}Ni irradiation (Hofmann *et al.* 1995b). Two more isotopes are reported: ^{267}110, produced (Ghiorso *et al.* 1995) in the irradiation of ^{209}Bi with ^{59}Co, which needs confirmation as the daughter decays

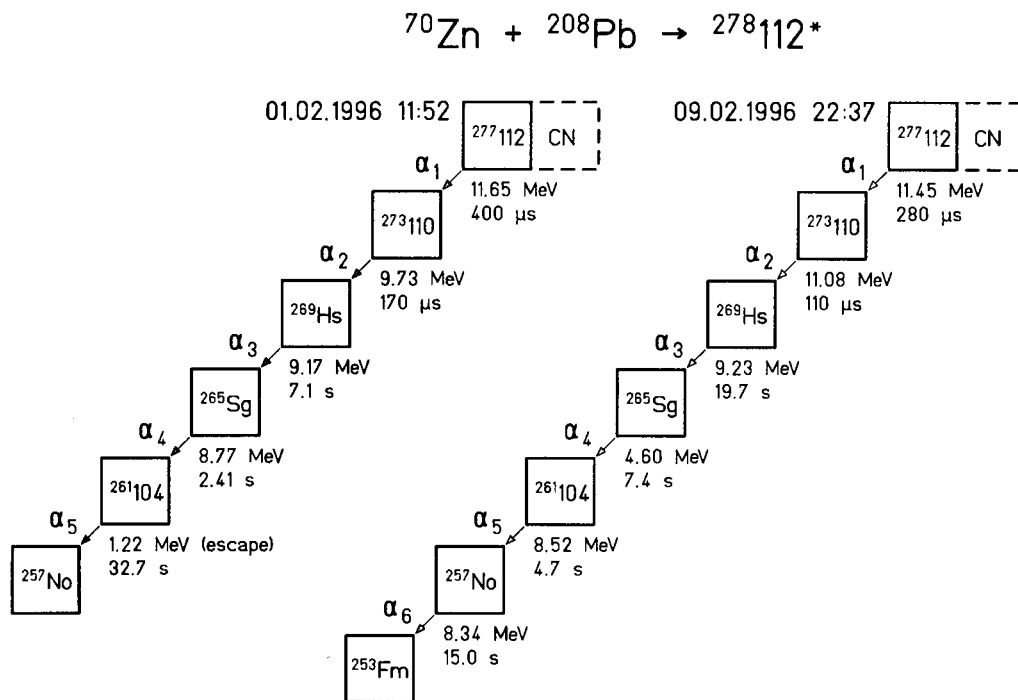Figure 2. The upper end of the periodic table.

2088 G. Münzenberg

Figure 3. The decay chains observed for element 112, the heaviest element known at present.

in the chain are not observed; and $^{273}110$ produced by irradiations (Lazarev *et al.* 1996) of ^{244}Pu with ^{34}S, a result which was confirmed when this isotope appeared in the decay chain of element 112.

Element 111 was created in the reaction ^{209}Bi(^{64}Ni,n). Altogether three α-chains were measured (Hofmann *et al.* 1995*b*). The observed isotope $^{272}111$ has a half-life of about 1.5 ms.

The heaviest element known today with proton number 112 was discovered in 1996 (Hofmann *et al.* 1996). In an experiment lasting 43 days irradiating ^{208}Pb with ^{70}Zn, the two decay chains displayed in figure 3 were observed. They show a remarkable signature. When the chain crosses the 162 neutron isotone, there appears a large gap of 1 MeV in the α-decay energies accompanied by strongly enhanced half-lives. This can be interpreted as the direct visibility of shell crossing.

(*b*) *The new shell region beyond rutherfordium*

The most striking results of recent heavy-element research are the dominance of α-decay in the heaviest elements, and the increasing half-lives for the neutron-rich nuclides. Both indicate an enhancement of nuclear stability in the region beyond rutherfordium.

Figure 4 shows the partial fission half-lives of the doubly even isotopes on a logarithmic scale plotted against the fissility parameter, a macroscopic scaling parameter characterizing the stability of a charged nuclear droplet against fission. From uranium to nobelium, half-lives decrease by over more than 20 orders of magnitude, from the age of the universe down to seconds in accordance with the expectations from
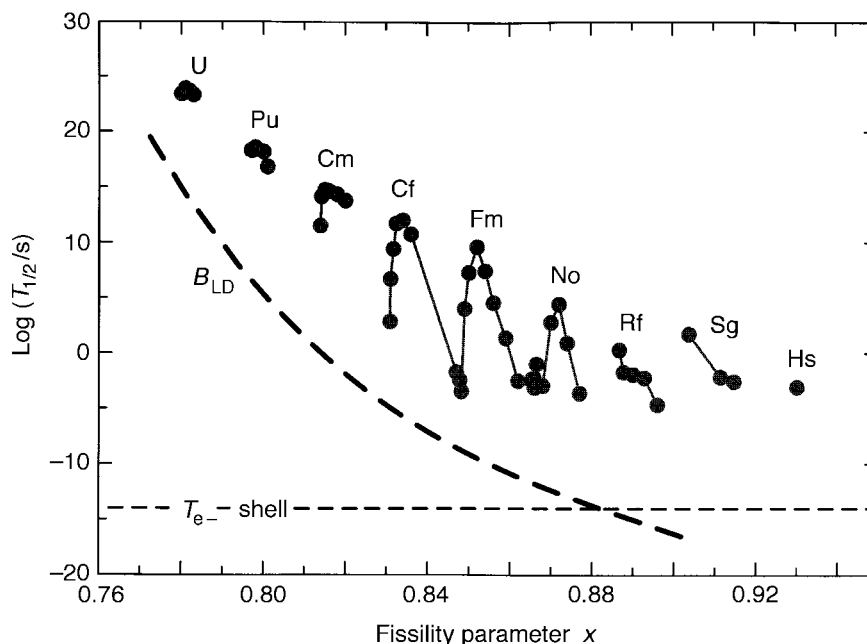
Figure 4. The partial fission half-lives of the doubly even isotopes from uranium to element 108.

the nuclear liquid drop model. The enhancement of fission half-lives in the isotopic chains of curium, californium, and fermium are due to a small shell effect at $N = 152$. The half-life systematics change completely at element 104. Half-lives become independent of the fissility parameter and stay almost constant. A comparison of the experimental data with the calculated liquid-drop half-lives shows an enhancement by 15 orders of magnitude for the heaviest elements, which must be attributed to microscopic stabilization.

If we define the half-life limit above which a chemical element can be accepted as the time needed for a nucleus to acquire its outer electrons (Barber *et al*. 1992), we arrive at 10^{-14} s. According to this definition, the nuclear chart would be terminated near element 104, but shell stabilization extends it up to the present experimental limit of $Z = 112$.

Figure 5 shows a typical shell barrier (Patyk *et al*. 1989; Sobiczewski 1996) for a transactinide nucleus in the example of $^{264}108$; it is single humped and thin. The liquid-drop part of the barrier, indicated by the dashed line, is zero. The outer part of the double-humped barrier characteristic of the actinides, sitting on top of the macroscopic barrier at large deformation, has dropped below the ground state with the vanishing droplet barrier and becomes ineffective.

The shell stabilization of the transactinides has its origin in a negative hexadecapole deformation in the ground state, as explained by theoretical models (Cwiok *et al*. 1983; Möller & Nix 1988, 1994; Patyk & Sobiczewski 1991). The trend of increasing shell-correction energies in the transactinide region is well reproduced by the theoretical models (Münzenberg *et al*. 1985; Münzenberg 1995; Sobiczewski 1996; Smolanczuk 1997), while the absolute values may differ by up to 1 MeV.

Figure 6 shows the full landscape of microscopic corrections between the shell closures at lead and element 114 calculated in the macroscopic–microscopic approach
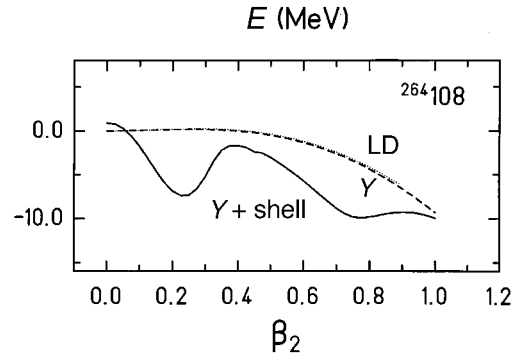
G. Münzenberg

E (MeV)

Figure 5. Calculated fission barrier for ^{264}108, a typical deformed-shell nucleus. The liquid drop (LD) barrier is indicated by the dashed line.
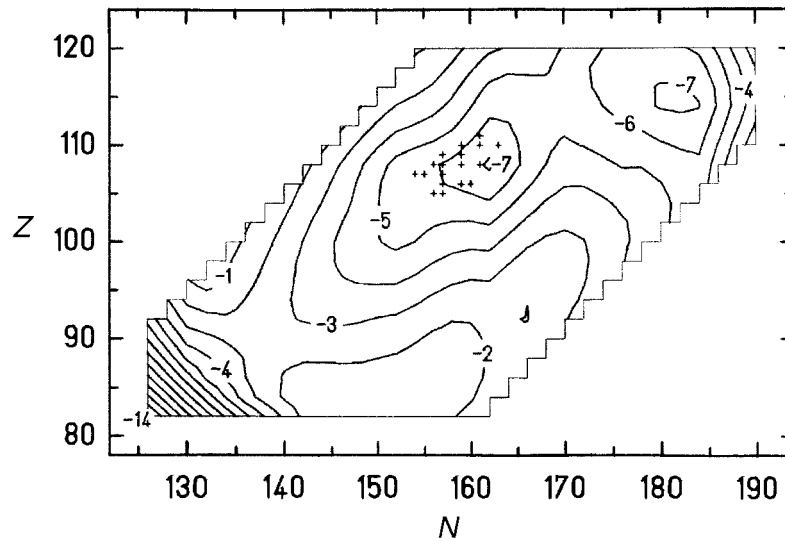

Figure 6. Shell-correction energies for the heavy and superheavy elements. The known isotopes of the heaviest elements are marked by crosses. More neutron-rich species can be accessed with radioactive beams.

with the Woods–Saxon single-particle potential (Smolanczuk 1997). The shell-correction energies show the steep minimum near the strong lead shell centred at ^{208}Pb, and a shallower minimum for the spherical superheavy shell closure at ^{298}114. The new shell region of deformed nuclei centred at ^{270}108 interconnects the transuranium elements and the spherical superheavies. The crosses mark the isotopes of the heaviest elements known today. They extend well into the new shell region. It should be noted here that the decay chains from ^{277}112 of figure 3 pass close by the stability maximum.

(c) New predictions

The macroscopic–microscopic theory reproduces the ground-state properties of the heaviest elements with sufficient precision. A comparison of the experimental
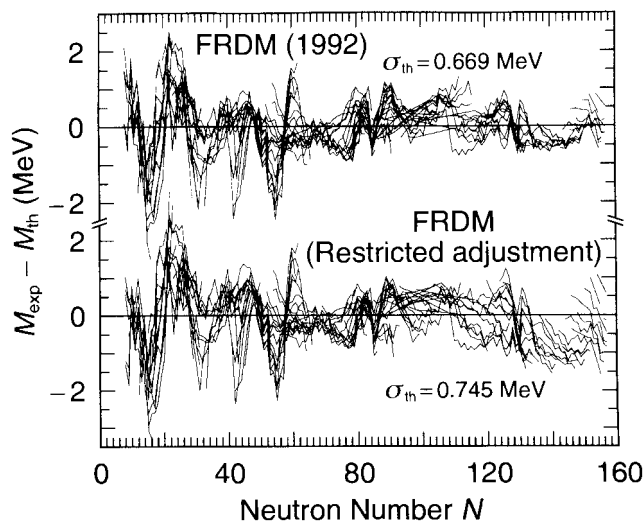
Figure 7. The differences between experimental masses and predictions from the macroscopic–microscopic model for two different parameter adjustments.

masses with the calculations suggests, however, some systematic deficiencies in the model for the heaviest known species (Münzenberg *et al.* 1987*b*) as shown in figure 7. The masses from the finite-range droplet model with microscopic corrections (Möller 1996) show a trend of systematically increasing deviations from experimental data towards the heaviest elements, even more dramatic for the restricted adjustment where only masses below $A = 208$ have been used for the parameter fit. This discrepancy has been interpreted as a distortion of the macroscopic surface, caused by the redistribution term of the droplet model which is related to the charge density in the nuclear droplet (W. J. Swiatecki, personal communication).

Recently, new calculations to predict the properties of the the heavy and superheavy elements have been performed in the self-consistent approach using Skyrme forces or the mean-field approach (Cwiok *et al.* 1996; Rutz *et al.* 1997). These calculations give different predictions for the proton shell closure at 114, 120, or 126 protons. Figure 8 shows examples (Cwiok *et al.* 1996) for the macroscopic–microscopic approach with the Woods–Saxon potential (WSP), and self-consistent Hartree–Fock calculations with Skyrme forces SKP and SLy7.

There are several half-life predictions for the heavy and superheavy elements, mostly from the macroscopic–microscopic theory for fission and α-decay (Sobiczewski 1996; Cwiok *et al.* 1996) and also including β-decay (Möller *et al.* 1997*a*). A half-life prediction from a self-consistent calculation (Cwiok *et al.* 1996) using the Skyrme interaction SKP for the doubly even isotopes of the superheavy elements is displayed in figure 9. For the known isotopes the prediction agrees with the experimental data.

The heavy nuclei are predicted to be α-emitters (Sobiczewski 1996). The longest-lived isotopes near $N = 184$ have partial α-half-lives exceeding 10^6 years. The hexadecapole stabilized region with maximum half-lives of 10^6 years forms a bridge between the upper end of the periodic table and the double shell closure, where half-lives of the elements above $Z = 124$ never drop below the order of microseconds, allowing one to approach the superheavy region stepwise with in-flight techniques,
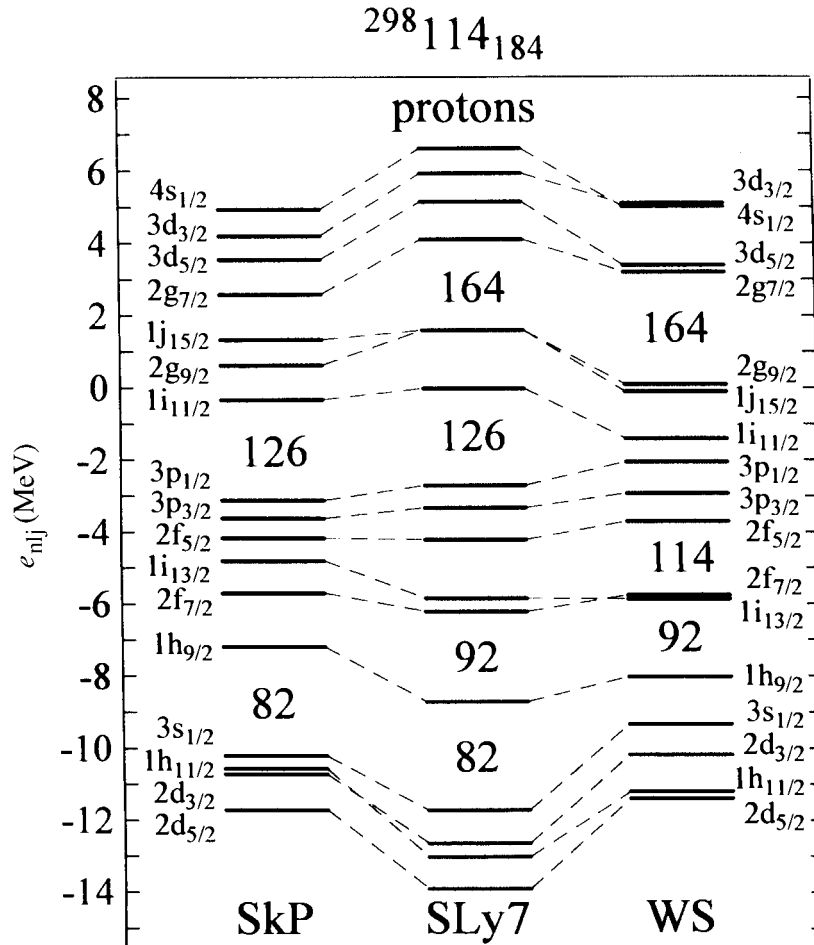
G. Münzenberg

$^{298}114_{184}$

Figure 8. The proton levels and shell gaps for Hartree–Fock calculation with the SKP and SLy7 parametrizations and the Woods–Saxon single-particle potential.

offering a rich field of neutron-rich nuclides for investigation, synthesized by using radioactive beams, and targets.

Half-lives of odd nuclei are longer due to the hindrance of fission and α-decay. Note that the calculations do not include β-decay, which will shorten the half-lives of the long-lived isotopes. For the heavy elements near $Z = 112$, the valley of β-stability comes close to $N = 184$ so β-decay of the long-lived species is excluded.

3. Perspectives for nuclear structure studies with radioactive beams

The neutron-rich, deformed-shell nuclei beyond $N = 162$ covering the region between the transuranium elements and the spherical superheavy shell closure offer a rich field for nuclear structure research with radioactive beams to investigate the behaviour of complex nuclear systems with balanced nuclear and Coulomb forces. The fact that the expected half-lives in this region exceed the order of seconds will open up this region for the continuation of chemical investigations and the application of new
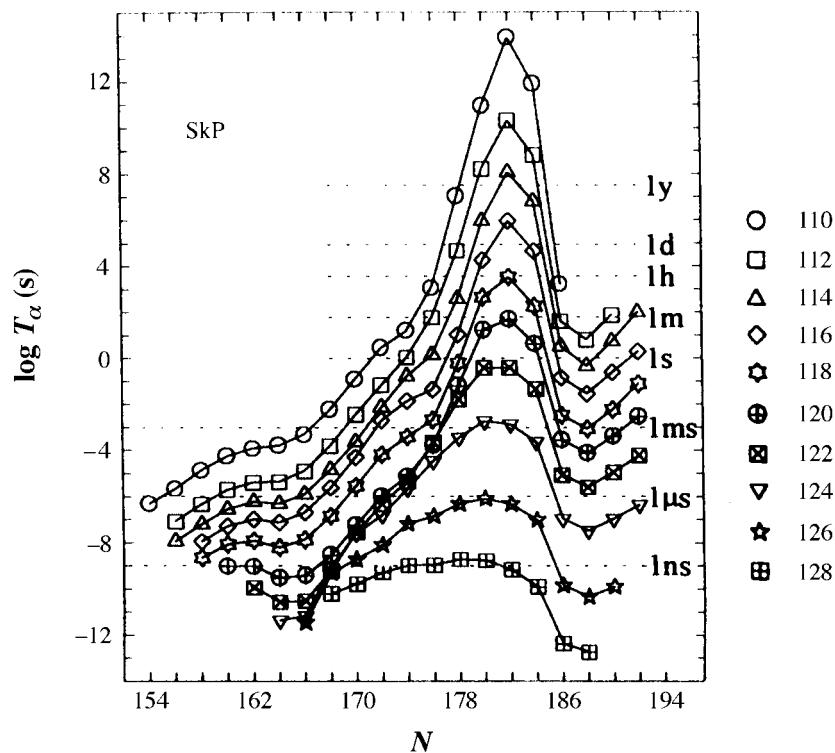
Figure 9. Partial α-half-lives for the superheavy elements $Z = 110$ to $Z = 128$ calculated with the SKP parametrization.

experimental techniques such as ion traps for direct mass measurements and laser spectroscopy to investigate nuclear and atomic properties.

Moreover, for the heaviest elements beyond 112, the decay chains end in neutron-rich isotopes which are unknown as yet, so the parent–daughter correlation method is not applicable for identification. The combination of heavy-element synthesis with stable and with neutron-rich radioactive beams would access this region directly on the one hand, and by overshooting on the other hand, and thus be compatible. Similar arguments hold for the nuclear structure investigations discussed in the following section.

(*a*) *Nuclear structure at large proton numbers and beyond $Z = 162$*

The nuclei beyond rutherfordium represent the species of nuclei beyond macroscopic stability. As the underlying macroscopic force is ineffective, already small shell gaps may create new shapes, so that a rich coexistence of nuclear deformations in all degrees of freedom may be observed. It has been debated whether there exists a spherical shell (Rigol 1997) at $N = 164$. In fact, the two decay chains of element 112, which are slightly different, might indicate such an effect. The second chain shows the largest energy step when crossing $N = 162$, the largest step in the first chain already appears in the first generation (Hofmann *et al*. 1996) when the decay
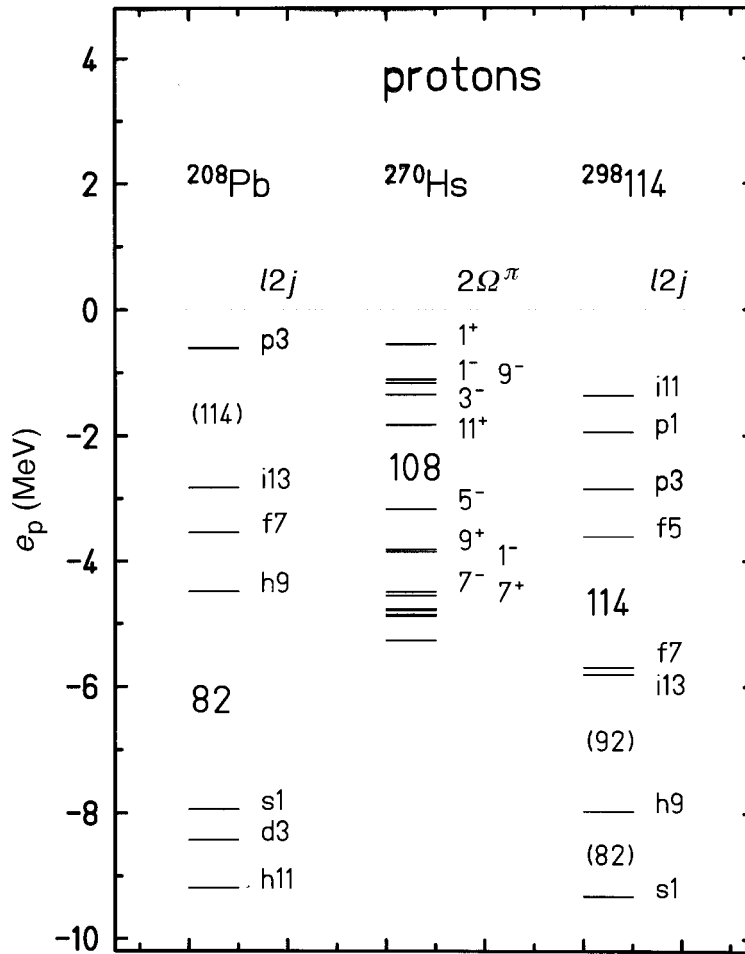
G. Münzenberg

Figure 10. Proton levels for ^{208}Pb compared to deformed and spherical superheavy nuclei (A. Sobiczewski, personal communication).

sequence crosses $N = 164$. A final answer to this question certainly needs further data along the isotones in the vicinity of the respective neutron numbers.

The elements at the upper end of the nuclear chart are the most complex nuclear systems. They have large level densities and high angular momenta. The complex structure of the heaviest elements is already visible in our data, showing a number of isomers. High- and low-spin orbits are coming close together and offer a rich field of interesting spectroscopy. Figure 10 shows the proton levels for the deformed and the spherical shell gaps for ^{270}Hs and ^{298}114 calculated with the Woods–Saxon single particle potential (A. Sobiczewski, personal communication). The figure shows that both gaps are about 2 MeV, less than that of the lead shell which amounts to more than 3 MeV. The level densities near the deformed shell are much higher than those around the spherical shell where low densities indicate an extended region of large shell corrections above $Z = 114$. This is visible in the map of shell-correction energies (figure 6).
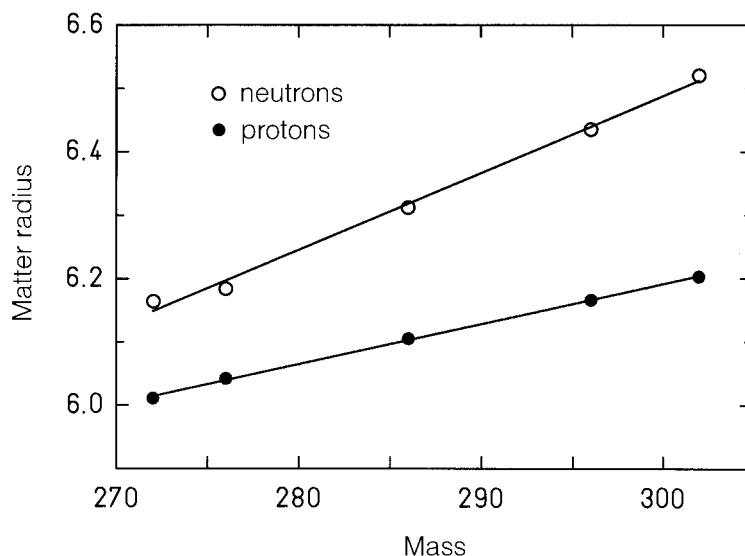
Figure 11. Calculated neutron and proton RMS radii for the isotopic chain of element 112 plotted against the mass number (H. Lenske, personal communication).

Because of their large volume the heaviest elements are the most appropriate objects to investigate bulk nuclear matter. Another interesting aspect is the study of nuclear structure under the influence of a strong Coulomb field. Self-consistent calculations (Cwiok *et al.* 1996; Rutz 1997; H. Lenske, personal communication) on the charge distribution in the superheavy nuclei show that the strong Coulomb forces in the heaviest elements create an enhanced charge density at the nuclear surface, affecting the high-spin orbits which are sensitive to the nuclear surface as they are pushed out from the centre of the nucleus due to the angular momentum barrier. The spin-orbit splitting at large mass values and its behaviour for the large diffuseness at the nuclear surface will show up in the level structure.

A mapping of the surface sensitive orbitals, such as isomeric states at high spin over an extended Z range along isotonic chains will help us to learn about the diffuseness of the proton surface. The systematic investigation of large isotopic chains will help us to understand the neutron–proton interaction at the surface, as the neutrons will follow the protons. These questions are related to the investigation of nuclear skins for the lighter nuclei. Figure 11 shows the charge and neutron radii of the $Z = 112$ isotopic chain (H. Lenske, personal communication) obtained from an HF-Bogoliubov calculation. Though the known isotope of element 112 is close to the proton drip-line, it already has a large neutron excess and forms a thin neutron skin, which grows to a thickness of 0.3 fm for the isotopes close to $N = 190$, close to β-stability. Such a skin thickness is comparable to that observed for extremely neutron-rich light nuclei, such as sodium. For increasing neutron number, charge radii increase due to pn coupling.

The question of where the spherical shell closures are located with respect to the superheavy elements can only be answered in experiments proceeding to continuously heavier elements. Valuable nuclear structure information, even on the nuclei at the very top, needs careful investigation of the lighter species which can be produced in sizeable quantities, as demonstrated in a recent experiment (Heßberger *et al.* 1997),

where more than a thousand atoms of $^{257}104$ were produced and detailed structure information was obtained from α-decay.

The neutron-rich species are predominantly important to extract structure information for the elements at the top of the nuclear table by climbing up the isotones. As the heavy elements at the top produced with stable beams tend to be increasingly neutron rich, the isotones in the lighter nuclei are only accessible with neutron-rich radioactive beams. Moreover, α-chains follow favoured transitions between similar spin states. Consequently, α-chains will populate nuclear states which may be different from those populated directly in the fusion process, as observed for element 108 in the element 110 decay chains (Hofmann *et al.* 1995*a*). Knowledge of the structure of the nuclei at the ends of the chains reveals some of the structure of the mother nuclei, but the full structure information about a nucleus is obtained by its study in direct production.

(*b*) *Extension of the deformed region and the end of the r-process*

One interesting question is how far the deformed island extends and how stability continues towards the spherical neutron shell in the elements around fermium, and how this affects nuclear half-lives. This question is related to the end of the r-process path. The neutron-rich region around fermium is of particular interest. In that region new fission modes, symmetric and bimodal fission, were discovered (Seaborg & Loveland 1990). The fission half-lives of fermium drop extremely quickly towards 158 neutrons and fall even below that of the transactinides. This was explained by a new fission path following compact shapes, and supported experimentally by a narrow symmetric mass distribution accompanied by a high total kinetic energy of the fragments. The distributions are influenced by the fragment shell structure of the the deformed shells along the fission path. This effect might affect fission half-lives strongly and totally compensate for shell stabilization.

4. Production of heavy and superheavy elements

(*a*) *Fusion of heavy systems*

Figure 12 displays the cross-sections for the production of the heaviest elements in terms of the proton number of the final residue. The heaviest known elements were produced by cold, heavy-ion fusion (Oganessian 1974). To produce elements with even proton number or odd proton number, lead or bismuth is irradiated with beams of ^{48}Ca, ^{50}Ti, ^{54}Cr, ^{58}Fe, ^{62,64}Ni, or ^{70}Zn. The cross-sections drop from the order of μmb for nobelium to one pb for element 112 and show a dependence on the projectile isospin. An increase of the isospin by 1 unit enhances the production cross-section by a factor of about five. The dots refer to $T_Z = 3$, circles to $T_Z = 4$. The excitation energies of the compound system for the maximum production cross-section are around 10 MeV for element 112 (figure 12, lower panel). For such cold systems the evaporation of one neutron is already sufficient to dissipate the excitation energy of the compound nucleus. The isospin dependence of the production cross-section can be explained most simply in terms of a decrease in excitation energy of the compound system at the barrier for the more neutron-rich projectiles.

The production cross-sections with actinide targets, ^{238}U and ^{244}Pu, in 5n and 4n reactions are indicated by filled squares. They are more than one order of magnitude
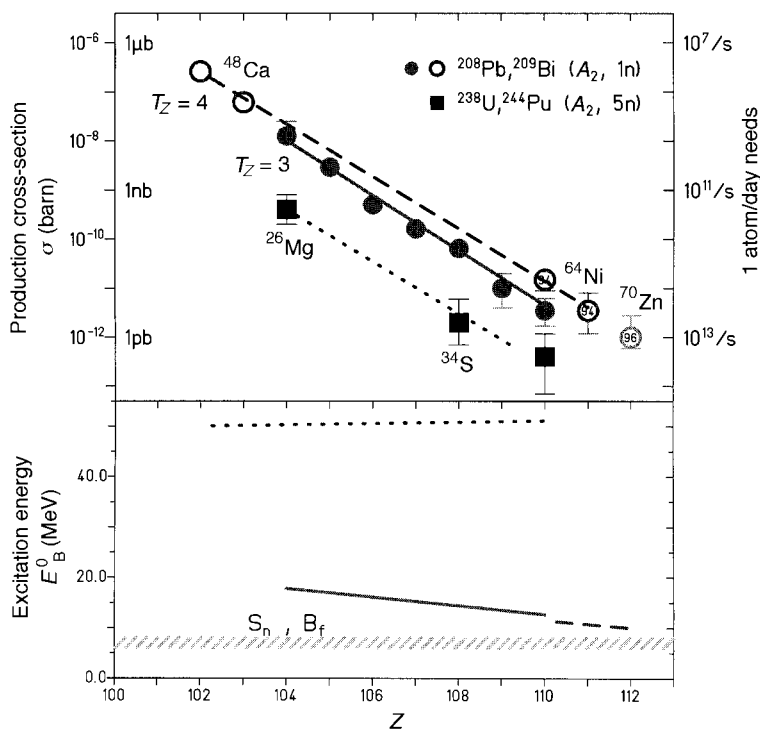
Figure 12. Production cross-sections for the heaviest elements plotted versus the proton number (upper panel) and excitation energies at the maximum production cross-section (lower panel). The beam intensities needed for the production of one atom per week are given on the left-hand scale.

below the cold fusion cross-sections. The heaviest element created with this type of reaction (Lazarev *et al.* 1996) is element 110.

The production of a heavy nucleus is a two-step process. In the first step, the projectile has to penetrate the Coulomb, or more precisely, the fusion barrier. Then the nuclear forces drive the dinuclear system from the contact configuration inside the fission saddle, which prevents the system from immediate disintegration. In general, the energy necessary for the projectile to overcome the Coulomb barrier is higher than the energy needed for the excess of binding energy in the heavy nucleus, so the compound system is excited. The excitation energy is dissipated by neutron evaporation and γ-emission. For the heaviest nuclei, there is a strong fission competition, which is more than three orders of magnitude higher than the probability for neutron emission.

The production cross-section for the fusion–evaporation reaction is

$$\sigma = \pi \lambda^2 \Sigma (2l + 1) \cdot T_l \cdot w_x,$$

where l is the angular momentum of the colliding system. The angular momentum limit for the fissile heavy elements is below 15 $\hbar$, corresponding to a cross-section of about 10 mb. Heavy elements are produced in central collisions. T_l is the angular-momentum-dependent transmission through the fusion barrier, and w_x the survival probability of the compound system after the evaporation of x neutrons. It can to a

first approximation be written as

$$w_x = (\Gamma_\mathrm{n}/\Gamma_\mathrm{f})^x$$

with $\Gamma_\mathrm{n}/\Gamma_\mathrm{f}$ characterizing the neutron-to-fission width. The idea of the cold fusion can immediately be derived from this relation: for the heaviest elements which are most fissile, the survival probability is expected to be highest if the system is formed cold and only one neutron is evaporated. This is shown by the data.

The small cross-sections for the production of the heavy elements cannot be explained by an infinitely small survival probability of the compound system. Models were developed to explain the losses in the entrance channel. The extra-push model developed for the fusion of massive nuclei predicts an enhancement of the fusion barrier for increasingly heavier systems due to dynamic losses in the dinuclear system on its way to fusion (Swiatecki 1982). The small cross-sections at the conventional fusion barrier can be explained in terms of an upshift of the barrier (Schmidt & Morawek 1991; Schmidt 1996).

Our experimental observation for the heavy elements shows the opposite behaviour. The excitation energies decrease towards the heavier elements: the production of element 112 is the coldest heavy-ion fusion ever observed. The macroscopic dynamics of the extra-push concept do not seem appropriate for describing the extremely cold production of closed-shell nuclei (Münzenberg 1988).

First attempts to explain qualitatively the influence of microscopic effects in the entrance channel on the production of heavy and superheavy elements have been made with the fragmentation theory (Sandulescu *et al.* 1976). This model predicts that the cold fusion of closed-shell nuclei, for example, the use of ^{208}Pb and corresponding projectiles is particularly favourable. Recently, calculations in the framework of the macroscopic–microscopic approach showed that the entrance channel fragment shell gaps are preserved far inside the contact point (Möller *et al.* 1997*b*).

New concepts, including microscopic effects in the entrance and exit channels, are being developed. The diffusion model uses a microscopic–macroscopic mode with temperature-dependent shell corrections to create a fusion pocket, the depth of which is determined by the excitation energy of the system on its way to fusion (Wada *et al.* 1997). The dinuclear system (DNS) concept assumes that fusion is achieved by transferring the nucleons shell by shell to build up the mononuclear system (Cherepanov *et al.* 1998). Both models stress the importance of microscopic effects. The losses in the fusion channel are explained by diffusion into the the fission valley. The influence of microscopic effects in the compound nucleus to enhance the survival in the de-excitation process has been investigated, but without positive result (Schmidt & Morawek 1991).

(*b*) *New possibilities with radioactive beams*

The problem of creating superheavy elements with stable beams is that one can never reach the $N = 184$ neutron shell closure in the vicinity of $Z = 114$. One idea, besides the use of neutron-rich exotic beams, is to profit from the increasing neutron excess in the heavier projectiles and to overshoot the proton number so that the neutron shell is crossed in the decay chains, as has been achieved for element 112. The beam intensities needed for the production of one atom per week are indicated in figure 12. If the cross-section systematics remain valid, the region beyond element

Table 1. *Expected intensities* (s^{-1}) *for neutron-rich radioactive beams*

SPIRAL	^{24}Ne	7×10^7
	^{44}Ar	5×10^7
PIAFE	^{78}Zn	10^8
	^{84}Ge	2×10^8
	^{94}Kr	2×10^9

114 needs beam intensities in excess of $10^{14}\ \text{s}^{-1}$. These intensities can be provided by the next-generation heavy-ion accelerator at GSI.

The first experiments on heavy-ion fusion with radioactive beams have already been started. Systems like ^{27,29,31}Al $+\ ^{197}$Au and ^{9,10,11}Be $+\ ^{209}$Bi were investigated. These pioneering experiments suffer from the poor quality of the data, which is partly due to weak beam intensities, so it is difficult to draw final conclusions. Nevertheless, new effects such as fusion enhancement with neutron-rich species seem to show up (Signorini 1997).

Table 1 shows the expected secondary beam intensities for two examples: SPIRAL, as a heavy-ion-based facility under construction; and PIAFE, a reactor-based project. They are of the order of $10^8\ \text{s}^{-1}$. The fission fragment beams from the reactor facility are fairly neutron rich. For the next generation facilities, such as the Munich reactor project and spallation facilities with $100\ \mu\text{A}$ proton beams of $1\ \text{GeV}$ intensities may be increased by three to four orders of magnitude (Münzenberg *et al*. 1997).

The extrapolation of the production rates for new elements beyond $Z = 112$ is difficult as the maximum of the production cross-section approaches two critical values: neutron-binding energy and the fission barrier of the compound nucleus. If the emission of one neutron is necessary to catch the dinuclear system inside the fission barrier, the position of the excitation function is fixed at its lower end by the neutron-binding energy. Going below it means that there is no dynamics left for the fusion process and no space for the neutron to evaporate. Cross-sections beyond $Z = 114$ may decrease faster than expected from the systematics of figure 12.

Similar arguments hold for the isospin enhancement to extrapolate the cold-fusion cross-sections with neutron-rich radioactive beams. On our present understanding isospin enhancement is only expected if there is enough room left for cooling the compound system, for example, for cold fusion in the heavy actinides. In the actinide-based fusion, large effects might be expected as the compound systems accessible with stable beams are produced with high excitation energy (figure 12). Radiative capture, though observed for lighter systems (Keller *et al*. 1986), has never been observed in the production of heavy elements, though several attempts have been made.

The domain of the neutron-rich beams will be beyond $N = 162$ in the actinide region below or up to element 104, where isospin enhancement should be effective and cross-sections are still in the nanobarn region. Hot fusion with actinide targets has enough room left for cooling and might be extremely attractive for light beams such as neon or magnesium plus curium to access elements 106 and 108, for example.

New fusion techniques need investigation. Fragmentation theory predicts three dominant paths to heavy elements (Singh *et al*. 1992): the cold fusion with lead targets, showing a deep valley, the actinide fusion, indicated by a weak valley, and in addition the symmetric fusion, or inverse fission, as yet unexplored. First experiments

on this reaction have been made (Stodel *et al*. 1997) in the investigation of ^{86}Kr on ^{130,136}Xe. The data could be explained in the framework of the statistical model. No upshift of the fusion barrier (Bass 1980) was found.

5. Nuclear transfer and reaction studies

Production of heavy elements by multinucleon transfer has been investigated in several experiments; it was the only tool to access neutron-rich actinides. Examples are the identification of ^{261,262}Lr and ^{262}No in the reactions of ^{18}O and ^{24}Ne with ^{264}Es. With the availability of neutron-rich beams, one certainly would come further (Schädel 1997) to the neutron-rich side.

The real power of first-generation secondary-beam facilities will be reaction studies. Radioactive beams extend our possibilities to investigate the importance of isospin and shell effects on fusion and transfer as they offer a rich choice of nuclides. Specifically, nuclear transfer as the doorway to fusion needs further attention. New experimental tools such as in-beam γ-spectroscopy with 4π germanium arrays would allow detailed studies and direct observation of the reaction channels not possible in the experiments up to now which, in the heavy-element region, were performed with nuclear chemistry.

6. Technical developments

(a) *Chemistry of the transactinides*

The investigation of the neutron-rich, long-lived, heavy elements produced with secondary beams needs the development of sensitive separation and detection techniques for long-lived species. The classical method of identification of an element, provided one can produce isotopes with sufficiently long half-life, is chemical separation.

Elements with half-lives exceeding 1 s are accessible to chemical investigation. A key question is the end of the Mendelejev systematics of the periodic table. The periodic table is understood in terms of successively filling electron shells when proceeding to heavier elements. For the heavy nuclei, however, the Coulomb forces of the nuclear core are so strong that the inner electrons become relativistic. Because the chemical behaviour of a chemical element strongly depends on the electronic configuration, these effects may influence the chemical properties. Such influence was investigated in the chemical behaviour of elements 105 and 106, respectively (Schädel 1997). The chemistry is based essentially on the study of the chemical behaviour of single atoms in volatile compounds by gas chromatography, or in aqueous solution by liquid chromatography. For these reasons chemistry is not an appropriate tool for discovering hitherto unknown elements, as their chemical properties are not predictable. On the contrary, chemistry has to rely on physical methods to identify a specific element in the chemical processing.

(b) *New in-flight techniques and detectors*

In-flight separation is the now established method for heavy-element research (Münzenberg 1997). The heavy fusion products recoiling from the target are separated in-flight with their full energy. The separation is fast. Separation times cor-
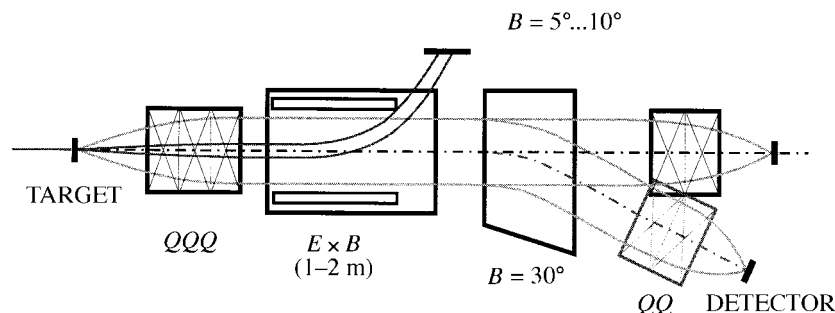
Figure 13. Schematic view of a recoil separator for applications with radioactive beams.

respond to the flight time through the separator which amounts to microseconds. Moreover, it is independent of chemical properties and efficient. With the recoil separator SHIP (Münzenberg 1974; Münzenberg *et al.* 1979), detection efficiencies for the heaviest elements are of the order of 50%.

SHIP is a two-stage velocity filter designed for heavy projectiles ($M \geqslant 40$) and high primary beam intensities of up to $10^{13}\ \text{s}^{-1}$. It can detect recoils with production cross-sections far below the nanobarn level. Separators for secondary-beam application have different requirements. Most of the facilities will use light beams and have much smaller intensities. Therefore, a compact separator with large acceptance is most appropriate. A large-aperture quadrupole doublet at the entrance to collect the recoils with large efficiency and one velocity filter combined with a dipole magnet are needed (figure 13). The dipole magnet has a variable deflection angle to be operated without charge dispersion at small angle or with increased dispersion in combination with the filter as recoil mass separator of moderate resolution.

The separated recoils are implanted into position-sensitive silicon detectors with their full energy, and identified by the α-decays following their implantation, observed at the position of implantation (Hofmann *et al.* 1984). Following the decay sequences to known transitions, they are identified unambiguously. With the example of element 109, it has been shown that this method was successful in identifying a new element on the decay of one single atom (Münzenberg *et al.* 1984*a*).

This technique works best for sequences of short-lived species, as they have the highest statistical significance. For long-lived isotopes at or near to closed shells, there are two strategies: as already discussed, the first is to overshoot this region. The decay chain will start at a short-lived isotope and run into the long-lived region. Then the respective detector position can be observed off-line until the chain continues.

To go directly into the long-lived region needs improved detection techniques permitting one to identify the recoil itself. As proton emission is not observed for the production of the heaviest elements, a determination of the mass number of the implanted recoil would be sufficient for identification. This can be achieved by time-of-flight and energy measurement. Silicon detectors have insufficient energy resolution due to the large pulse height defect for the heavy and slow fragments (Münzenberg *et al.* 1984*a*). The recently developed bolometric detectors have been shown to provide energy resolution (Meier *et al.* 1996) of the order of 10^{-3}, which is sufficient for mass identification in the $M = 300$ region. These detectors work at liquid helium temperatures, and measure the temperature increase induced by the heat deposited in a crystal. They can also detect α-decay with a resolution of better than 50 keV.

(*c*) *Trapping and laser techniques*

The combination of ion traps with recoil separators will open up new possibilities such as high-precision mass measurements and laser spectroscopy to determine deformations or ionization potentials. An example is the SPIG ion guide (Fujitaka *et al.* 1997) coupled to a gas-filled recoil separator. A combination of an RFQ ion guide to catch the recoils, a cooler trap and a precision trap is being developed (Habs *et al.* 1997) to operate in combination with SHIP. It would be interesting to investigate how the charge distribution in the nuclei would show up in the isotope shifts.

7. Conclusion

Recent heavy-element research led to the discovery of deformed, shell-stabilized nuclei, creating an extended region of enhanced stability which connects the transuranium region to the magic proton number 114, already closely approached with the discovery of element 112. While new elements beyond $Z = 114$ will, according to our present knowledge, only be accessible with intense beams deliverable from high-current accelerators, the region beyond $N = 162$, accessible with neutron-rich beams, will offer a rich field for nuclear structure studies with new phenomena expected. The long half-lives will allow the application of new methods for high-precision studies of nuclear and atomic properties, and chemistry.

References

Argonne 1995 The Argonne Radioactive Beam Project. *Int. Rep. Argonne Natn. Lab.* Argonne, USA.

Armbruster, P. 1985*a* *A. Rev. Nucl. Sci.* **25**, 135–194.

Armbruster, P. 1985*b* In *Nuclei to Stars, Proc. 91st Corso Soc. Italiana di Fisica, Bologna, Italy*, pp. 222–249. Amsterdam: North-Holland.

Barber, R. C., Greenwood, N. N., Hryenkiewicz, A. Z., Jeannin, Y. P., Lefort, M., Sakai, M., Ulehla, I., Wapstra, A. A. & Wilkinson, D. H. 1992 *Prog. Part. Nucl. Phys.* **29**, 453.

Bass, R. 1980 Lecture Notes in Physics, vol. 117, p. 420. Berlin: Springer.

Bohr, N. & Wheeler, J. A. 1939 *Phys. Rev.* **56**, 426–450.

Cherepanov, E. A., Adamian, G. G., Antonenko, N. V., Nasirov, A. K. & Volkov, V. V. 1998 (In the press.)

Cwiok, S., Pashkevich, V. V., Dudek, J. & Nazarewicz, W. 1983 *Nucl. Phys.* A **410**, 254.

Cwiok, S., Dobaczewski, J., Heenen, P. H., Magierski, P. & Nazarewicz, W. 1996 *Nucl. Phys.* A **611**, 211.

Demin, A. G., Tretyakova, S. P., Utyonkov, V. K. & Shirokovsky, I. V. 1984 *Z. Phys.* A **315**, 197–200.

Feenberg, E. 1939 *Phys. Rev.* **55**, 504–505.

Fizet, E. O. & Nix, J. R. 1972 *Nucl. Phys.* A **193**, 647–671.

Fujitaka, S. (and 10 others) 1997 *Nucl. Instrum. Meth.* B **126**, 386.

Geissel, H., Münzenberg, G. & Riisager, K. 1995 *A. Rev. Nucl. Part. Sci.* **45**, 163–203.

Ghiorso, A. (and 28 others) 1995 *Nucl. Phys.* A **583**, 861.

Greenwood, N. N. 1997 *Pure Appl. Chem.* **96**, 197–184.

Habs, D. *et al.* 1997 *Int. Comm. GSI.*

Heßberger, F. P. (and 10 others) 1997 *Z. Phys.* A **359**, 415–425.

Hofmann, S. 1997 *Rep. Prog. Phys.* **61**, 639–689.

Hofmann, S., Münzenberg, G., Heßberger, F. P. & Schött, H. J. 1984 *Nucl. Instrum. Meth.* **223**, 312–318.

Hofmann, S. (and 12 others) 1995*a* *Z. Phys.* A **350**, 277.

Hofmann, S. (and 12 others) 1995*b* *Z. Phys.* A **350**, 281.

Hofmann, S. (and 11 others) 1996 *Z. Phys.* A **354**, 229.

Hofmann, S. (and 10 others) 1997 *Z. Phys.* A **358**, 377–378.

Keller, J. G., Schmidt, K.-H., Heßberger, F. P., Münzenberg, G., Reisdorf, W., Clerc, H. G. & Sahm, C. C. 1986 *Nucl. Phys.* A **452**, 173–204.

Kubono, S., Kobayashi, T. & Tanihata, I. (eds) 1997 *Proc. Fourth Int. Conf. on Radioactive Nuclear Beams, Omiya, Japan, 1996. Nucl. Phys.* A **616**.

Lazarev, Yu. A. (and 17 others) 1995 *Phys. Rev. Lett.* **78**, 1903–1906.

Lazarev, Yu. A. (and 16 others) 1996 *Phys. Rev.* C **54**, 620–625.

Meier, J., Chulkov, L., Egelhof, P., Fischer, C., Henning, W., Kienlin, A. V., Kirchner, G., Kraus, G. & Weinbach, A. 1996 *Nucl. Instrum. Meth.* A **370**, 259.

Meitner, L. & Frisch, O. 1939 *Nature* **143**, 239–240.

Möller, P. 1996 Int. Rep. GSI, Darmstadt, Germany.

Möller, P. & Nix, J. R. 1988 *At. Data Nucl. Data Tables* **39**, 213.

Möller, P. & Nix, J. R. 1994 *J. Phys.* G **20**, 1681.

Möller, P., Nix, J. R. & Kratz, K. L. 1997*a* *At. Data Nucl. Data Tables* **66**, 131–343.

Möller, P., Nix, J. R., Armbruster, P., Hofmann, S. & Münzenberg, G. 1997*b* *Z. Phys.* A **359**, 251–255.

Mosel, U. & Greiner, W. 1969 *Z. Phys.* **222**, 261–282.

Münzenberg, G. 1974 *Int. J. Mass Spectr. Ion Phys.* **14**, 363–378.

Münzenberg, G. 1988 *Rep. Prog. Phys.* **51**, 57–104.

Münzenberg, G. 1995 *Radiochimica Acta* **70/71**, 193.

Münzenberg, G. 1997 In *Experimental techniques in nuclear physics* (ed. W. Greiner & D. N. Poenaru), pp. 375–424. Berlin: De Gruyter.

Münzenberg, G. 1998 In *Int. Symp. on Nuclear and Particle Physics with High Intensity Proton Accelerators, Tokyo, Japan, 1996*, pp. 215–222. Singapore: World Scientific.

Münzenberg, G., Faust, W., Hofmann, S., Armbruster, P., Güttner, K. & Ewald, H. 1979 *Nucl. Instrum. Meth.* **161**, 65–82.

Münzenberg, G., Armbruster, P., Heßberger, F. P., Hofmann, S., Poppensieker, K., Reisdorf, W., Schneider, J. R. H., Schneider, W. F. W. & Schmidt, K.-H. 1982 *Z. Phys.* A **309**, 89–90.

Münzenberg, G. (and 12 others) 1984*a* *Z. Phys.* A **315**, 145–158.

Münzenberg, G. (and 11 others) 1984*b* *Z. Phys.* A **317**, 235–236.

Münzenberg, G. (and 12 others) 1985 *Z. Phys.* A **322**, 227–235.

Münzenberg, G. (and 15 others) 1987*a* *Z. Phys.* A **324**, 489–490.

Münzenberg, G. (and 17 others) 1987*b* *Z. Phys.* A **328**, 49–59.

Münzenberg, G. (and 18 others) 1988 *Z. Phys.* A **330**, 435–436.

Münzenberg, G., Geissel, H. & Scheidenberger, C. (eds) 1997 *Proc. Int. Conf. on Electromagnetic Isotope Separators and Techniques Related to their Application, Bad Dürkheim, Germany, 1996. Nucl. Instrum. Meth.* B **126**.

Oganessian, Y. Ts. 1974 Lecture Notes in Physics, vol. 33, pp. 221–252. Berlin: Springer.

Patyk, Z. & Sobiczewski, A. 1991 *Nucl. Phys.* A **533**, 132.

Patyk, Z., Sobiczewski, A., Armbruster, P. & Schmidt, K. H. 1989 *Nucl.Phys.* A **491**, 267.

Randrup, J., Larsson, S. E., Möller, P., Sobiczewski, A. & Lukasiak, A. 1974 *Physica Scr.* A **10**, 60–64.

2104 *G. Münzenberg*

Randrup, J., Larsson, S. E., Möller, P., Nilsson, S. G., Pomorski, K. & Sobiczewski, A. 1976 *Phys. Rev.* C **13**, 229–239.

Rigol, J. 1997 *Phys. Rev.* C **55**, 972–973.

RIKEN 1994 The RIKEN Upgrade. Int. Rep. RIKEN, Tokyo, Japan.

Rutz, K. 1997 Thesis, Universität Frankfurt/Main, Germany.

Rutz, K., Bender, M., Bürvenich, T., Schilling, T., Reinhard, P.-G., Maruhn, J. A. & Greiner, W. 1997 *Phys. Rev.* C **56**, 238–243.

Sandulescu, A., Gupta, R. K., Scheid, W. & Greiner, W. 1976 *Phys. Lett.* B **60**, 225.

Schädel, M. 1996 In *Proc. Int. Worksop on Research with Fission Fragments, Benediktbeuren, Germany, 1996*, pp. 104–109. Singapore: World Scientific.

Schädel, M. (and 17 others) 1997 *Nature* **388**, 3.

Schmidt, K.-H. 1996 In *Proc. Int. Worksop on Research with Fission Fragments, Benediktbeuren, Germany*, pp. 110–115. Singapore: World Scientific.

Schmidt, K.-H. & Morawek, W. 1991 *Rep. Prog. Phys.* **54**, 949–1003.

Seaborg, G. T. & Loveland, W. D. 1990 *The elements beyond uranium.* New York: Wiley.

Signorini, C. 1997 *Nucl. Phys.* A **616**, 262.

Singh, S., Gupta, R. K., Scheid, W. & Greiner, W. 1992 *J. Phys.* G **18**, 1243–1257.

Smolanczuk, R. 1997 Preprint SINS/TH/1997, Soltan Institute for Nuclear Studies, Warsaw, Poland. *Phys. Rev.* C **56**, 812–824.

Sobiczewski, A. 1996 *Phys.-Uspekhi* **39**, 885–889.

SPIRAL 1994 The SPIRAL Project. Int. Rep. GANIL, Caen, France.

Stodel, C., Hofmann, S., Heßberger, F. P., Vinov, V., Sagaidak, R. N., Popeko, A. G., Oganessian, Yu. Ts., Lavrentjev, A. Yu. & Yeremin, A. V. 1997 *A. Rep. GSI* **1996**, 17.

Swiatecki, W. J. 1982 *Nucl. Phys.* A **376**, 275–291.

Wada, T., Arimoto, Y., Tokuda, T., Ohta, M. & Abe, Y. 1997 *Nucl. Phys.* A **616**, 446.